

Tennessee Valley Authority
Division of Water Management
Water Systems Development Branch

MODEL STUDY OF THE WATTS BAR RHR SUMP

Report No. WM28-1-85-101

Prepared by
Theodoric G. Fain

Norris, Tennessee
March 1979

Basket # 50-390
Control # 7905290390
Date 5/23/79 of Document
REGULATORY DOCUMENT FILE

7905290399

CONTENTS

	<u>Page</u>
INTRODUCTION	1
PROTOTYPE DESCRIPTION	2
MODEL DESCRIPTION	5
MODEL SIMILITUDE	8
Model Limits	8
Kinematic and Dynamic Similarity	8
Model Screens	12
Sump Loss Coefficient	14
MODEL TESTS	17
RESULTS	17
Sump Interior	17
Sump Inlet and Vicinity	17
Sump Loss Coefficient	21
CONCLUSIONS	24
REFERENCES	25

LIST OF TABLES

<u>Table No.</u>	<u>Title</u>	<u>Page</u>
1	Range of Prototype and Model Reynolds Numbers	11
2	Comparison of Model and Prototype Screens	14
3	Schemes Tested with Final Design and Results	19

LIST OF FIGURES

<u>Figure No.</u>	<u>Title</u>	<u>Page</u>
1	Model Limits (Watts Bar Unit 1)	3
2	Original Containment Sump Design	4
3	Overall View of Model	6
4	View of Sump	6
5	Loss Coefficient for Screens	13
6	Illustration of Sump Loss Coefficient Calculation	16
7	Arbitrary Vortex Strength Scale	18
8	Final Design with Vortex Suppressors and Other Modifications	20
9	Details of Cruciform	22
10	Sump Loss Coefficient Reynolds Number Dependency	23

INTRODUCTION

The containment sump design for Watts Bar Nuclear Plant has been tested by TVA at the Engineering Laboratory, Norris, using a 1:4 scale physical model. The original design was tested for possible trapped air in the sump during initial filling and for air-drawing vortices during operation. Where necessary, recommendations were made for improving the design. The sump pressure loss coefficient with the final recommended design was determined empirically for use in pump net positive suction head calculations. This report describes the model and presents test results and recommendations.

PROTOTYPE DESCRIPTION

The containment sump inlet is located in the 8-foot high passageway under the refueling canal, as shown in Figure 1. The annular shape of the containment area (elevation 702.78) allows water to approach the sump from two directions simultaneously, passing in both cases through screened trashracks ($\frac{1}{4}$ -inch mesh screen welded to standard floor grating) at the entrances to the passageway. Water from the two 14-inch drain holes in the floor of the refueling canal is piped outside the passageway to avoid jetting directly into the sump inlet. The water surface in the containment area bounded by the crane wall, reactor shield wall and refueling canal walls is at elevation 716.0 during withdrawal through the sump, at which time the passageway under the refueling canal is fully submerged.

The sump, shown as initially designed in Figure 2, has two discharge pipes which can be operated independently. A $\frac{1}{4}$ -inch mesh screen is located in front of the pipe entrances. The maximum water temperature during withdrawal is 160°F. The pump design flow rate is 8500 gpm per pipe. The maximum flow rate through the sump was estimated as 19750 gpm. This flow rate was used throughout the model study, except where noted.

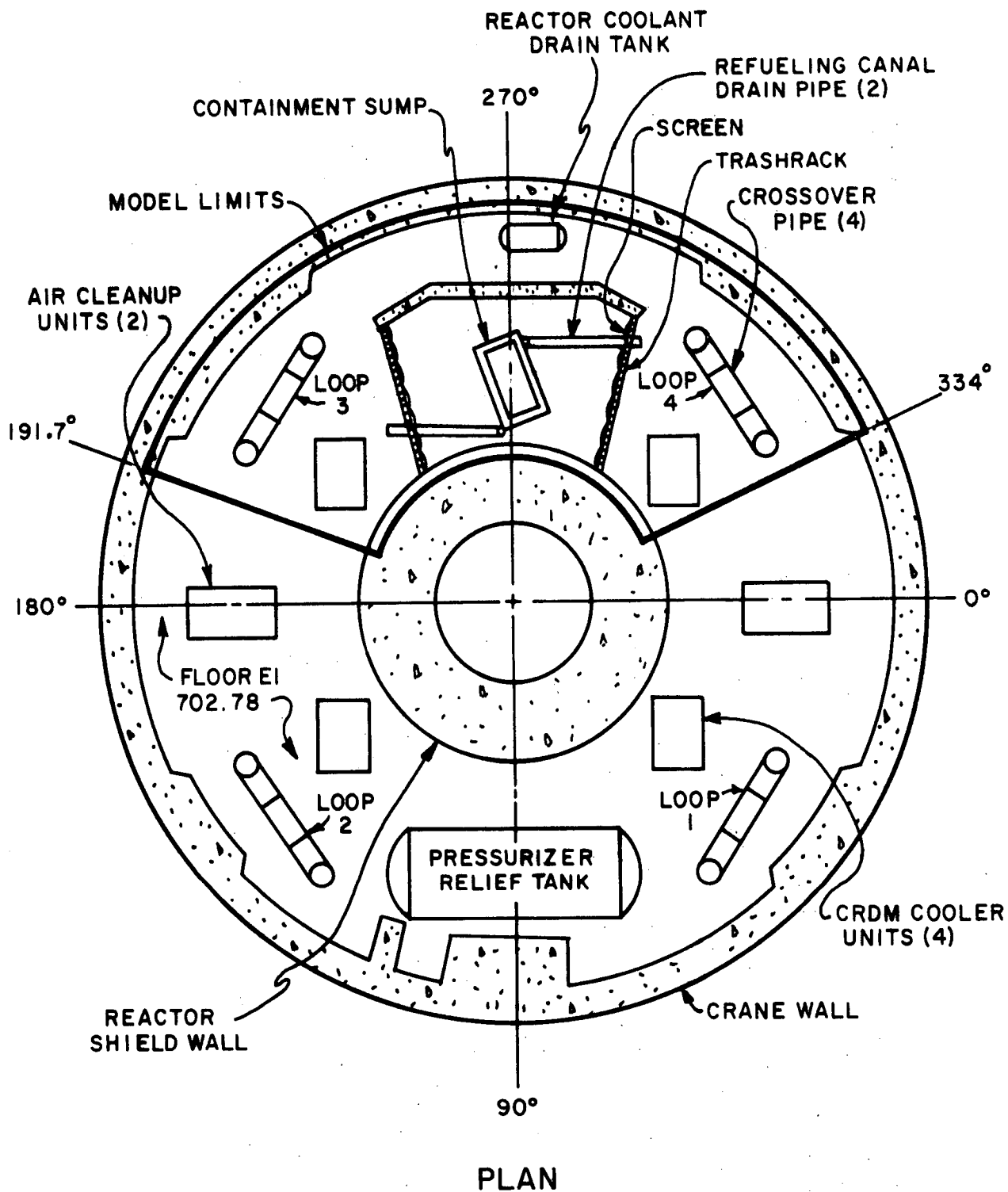


Figure 1: Model Limits (Watts Bar Unit 1)

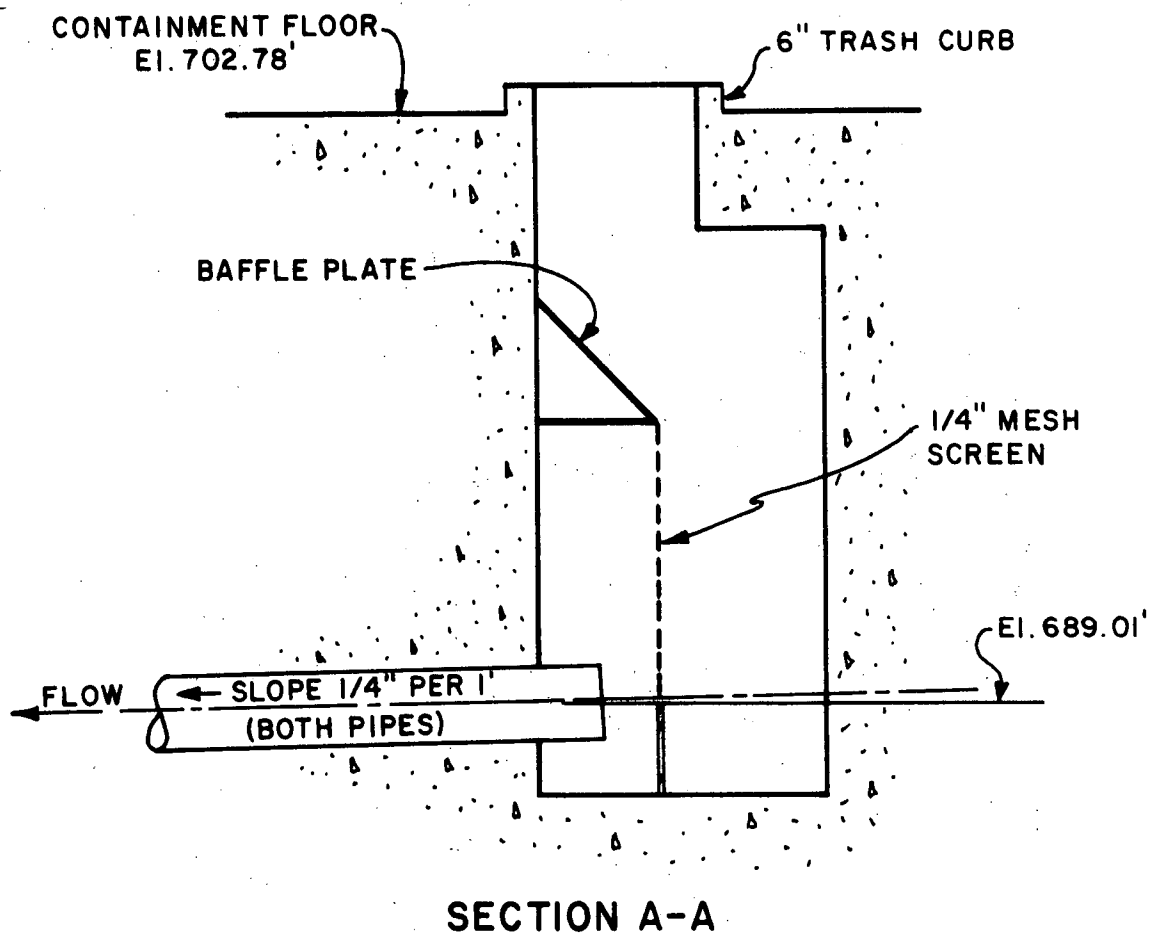
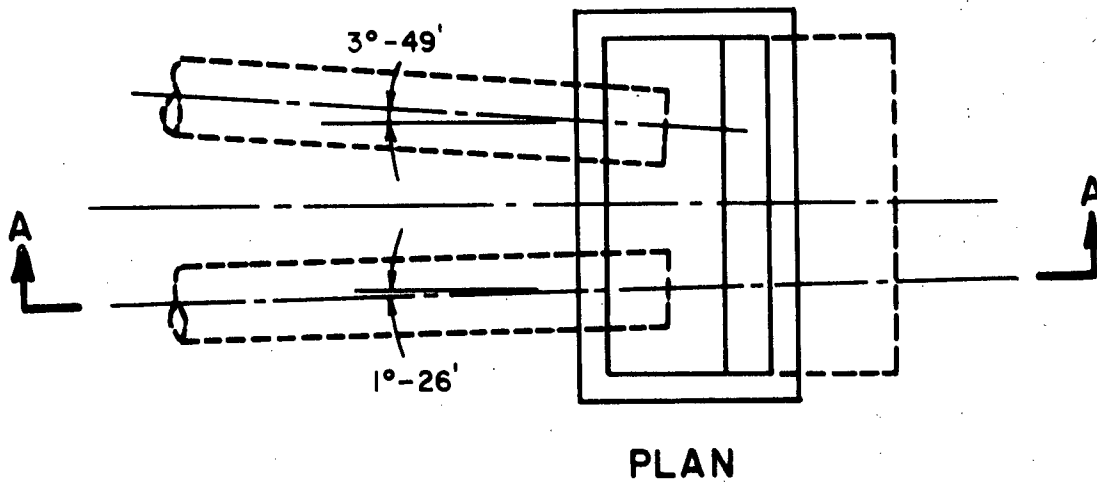


Figure 2 : Original Containment Sump Design, Unit 1
(Units 1 and 2 Opposite Hand)

MODEL DESCRIPTION

The model had the orientation of Unit 1 (Units 1 and 2 are opposite hand but otherwise identical) and included the containment sump, the two discharge pipes leading from the sump, the passageway under the refueling canal, and a portion of the containment area. The portion of containment (elevation 702.78) included extended from Steam Generator No. 3 (azimuth 191.7) clockwise to Steam Generator No. 4 (azimuth 334.0), as shown in Figure 1. Within this space bounded by the floor, the crane wall, the reactor shield wall, the refueling canal walls, and elevation 716.0, all structures larger than 4 inches across which could affect the flow were modeled. Figure 3 shows an overall view of the model. Figure 4 shows the sump and a portion of each discharge pipe. The crane wall and other walls and surfaces required to be transparent for flow visualization were made of clear acrylic plastic.

Water was supplied to the model through perforated plates at both ends of the model (azimuths 191.7 and 334.0), through pipes leading from the two drain holes in the floor of the refueling canal, and through a movable pipe which could be placed anywhere in the containment. Flow rates for each of these sources were independently controlled by valves and measured with calibrated orifice meters. All water supplied to the model was withdrawn through the sump by a pump and recirculated directly back to the model. The water level in the containment was controlled by regulating the volume of water in the model and piping system.

For testing at water temperatures higher than ambient, five 2.5 kW resistance heating elements were installed behind each of the

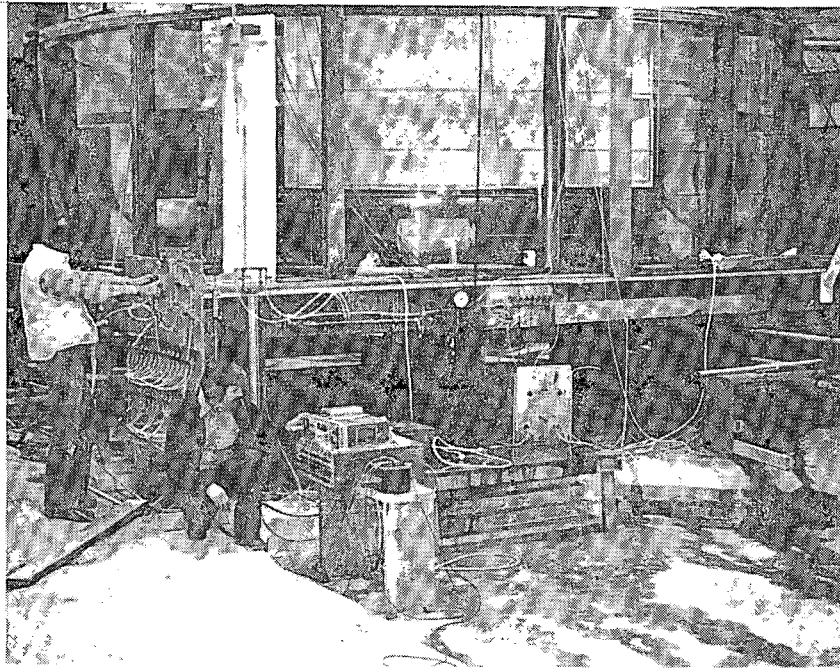


FIGURE 3: OVERALL VIEW OF MODEL

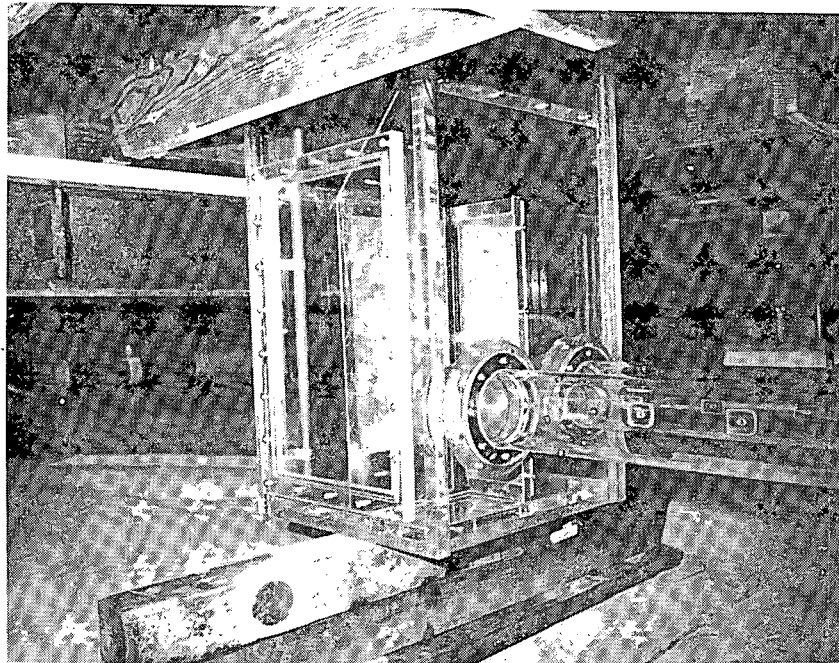


FIGURE 4: VIEW OF SUMP

perforated plates at the ends of the model. The maximum water temperature possible was approximately 130°F.

MODEL SIMILITUDE

Model Limits

Preliminary tests were performed to determine if sufficient lengths of the annular-shaped containment area on both sides of the refueling canal had been included in the model. These lengths would be sufficient if equipment in the flow outside the model limits would have no effect on flow patterns at the sump. To show this, water was supplied alternately to one end of the model only, to the opposite end, and to both ends simultaneously. In each case, the flow pattern in the vicinity of the sump was observed with the aid of injected dye. No noticeable change in the flow pattern near the sump occurred. Hence, it was concluded that flow patterns at the sump were being controlled by conditions relatively near the sump and not by the outer limits of the model.

Kinematic and Dynamic Similarity

Because of the predominance of gravitational and inertial forces in the flow processes involved, kinematic and dynamic similitude were achieved primarily by equating the Froude numbers¹ of the model and prototype. The Froude number, representing the ratio of gravitational to inertial forces, was defined as

$$F = V/\sqrt{gs} \quad (1)$$

where

V = discharge pipe velocity

g = gravitational acceleration

s = submergence of the discharge pipe centerline below the free surface

and was made equal in the model and the prototype:

$$F_r = F_m / F_p = 1 \quad (2)$$

where subscripts m, p, and r represent model, prototype, and ratio between model and prototype, respectively. Velocity, flow rate, and time, V, Q, and t, respectively, were expressed in terms of the chosen geometric scale:

$$L_r = L_m / L_p = 1/4$$

where L refers to length. By use of Equations 1 and 2 with $g_r = 1$,

$$V_m = L_r^{1/2} V_p = 0.5 V_p$$

$$Q_m = L_r^{5/2} Q_p = 0.03125 Q_p$$

$$t_m = L_r^{1/2} t_p = 0.5 t_p$$

The flow field depended to a lesser extent on viscous and possibly surface tension effects. The relative magnitudes of these forces to fluid inertia were reflected in the Reynolds and Weber numbers, defined respectively as

$$R = VD/\nu$$

and

$$W = \rho V^2 s / \sigma$$

where

V = discharge pipe velocity

D = discharge pipe diameter

ν = kinematic viscosity

ρ = density

σ = surface tension

s = submergence of discharge pipe centerline below the free surface.

Because the model flow rate had to be determined on the basis of equal model and prototype Froude numbers, the Reynolds and Weber numbers could not have the same values they would have in the prototype. Any deviation in similitude of the flows attributable to viscous and surface tension forces was called scale effect. Surface tension effects were small because vortices with significant free surface curvature were not present in the model². Vortex formation was therefore predominantly a function of Froude number, with possibly a minor scale effect because of the reduced model Reynolds number. The model Reynolds numbers were high enough that the flow in the model was fully turbulent, i.e., in the same regime as that in the prototype. Therefore, scale effects due to viscous forces were negligible. This condition was assured by employing the following modeling techniques:

- (1) The large model Reynolds numbers were achieved by choosing a large geometric scale ratio for the model (1:4).
- (2) The model was operated at pipe velocities higher than Froude scale to increase the model Reynolds number, but without excessively violating Froude scaling criterion (F_r maximum = 2.6).

- (3) The model was operated at water temperatures higher than ambient to further increase the model Reynolds number ($\theta_{\max} = 130^{\circ}\text{F}$).
- (4) The model was operated at water levels lower than the design minimum to exaggerate the propensity for vortex formation.

The Reynolds number ranges of the model and prototype are given in Table 1.

TABLE 1
RANGE OF PROTOTYPE AND MODEL IR
($Q_p = 9875$ gpm per pipe)

<u>Temp.</u> °F	<u>Prototype IR</u>	<u>Model IR</u>		
		$F_r=1$	$F_r=2$	$F_r=2.6$
60°	1.59×10^6	1.99×10^5	3.97×10^5	5.17×10^5
130°	3.47×10^6	4.33×10^5	8.66×10^5	1.12×10^6
160°	4.38×10^6	--	--	

Details of the model scale selection were given in the Sequoyah³ report. In accordance with common practice⁴, the model was operated with velocities in the discharge pipes higher than Froude scale and observed for vortexing tendencies. The highest velocity obtained in the model was 17.4 ft/sec; the velocity in the prototype at maximum pipe discharge will be about 13.4 ft/sec. Under these conditions, V_m/V_p was approximately 1.3. Also, the water temperature in the model, usually in the range 40° to 90°F, was raised to about 130°F for some tests.

Model Screens

Screen material for the model was selected which had the same pressure loss coefficient as the prototype screen, with the wire diameter and opening width as near 1:4 scale as possible. Thus the effect of the two model screens on pressure loss and on velocity profile modification were properly simulated. The pressure loss coefficient for the screens, defined as

$$K = \Delta H / (v_s^2 / 2g)$$

was computed from the expression^{5,6}

$$K = 1 / (3\epsilon^2) [103.4(d \cdot a)^2 / R_e + 6.24 d / \ell]$$

where

ΔH = pressure drop through screen

v_s = unobstructed upstream velocity

d = wire diameter

ℓ = width of opening in screen

a = ratio of the sum of surface areas of the individual strands of wire which make up the screen to the total volume occupied by the screen, including both wires and voids

R_e = Reynolds number based on the wire diameter and the unobstructed upstream velocity

ϵ = ratio of the sum of volumes of the voids in the screen to the total volume occupied by the screen, including both wires and voids

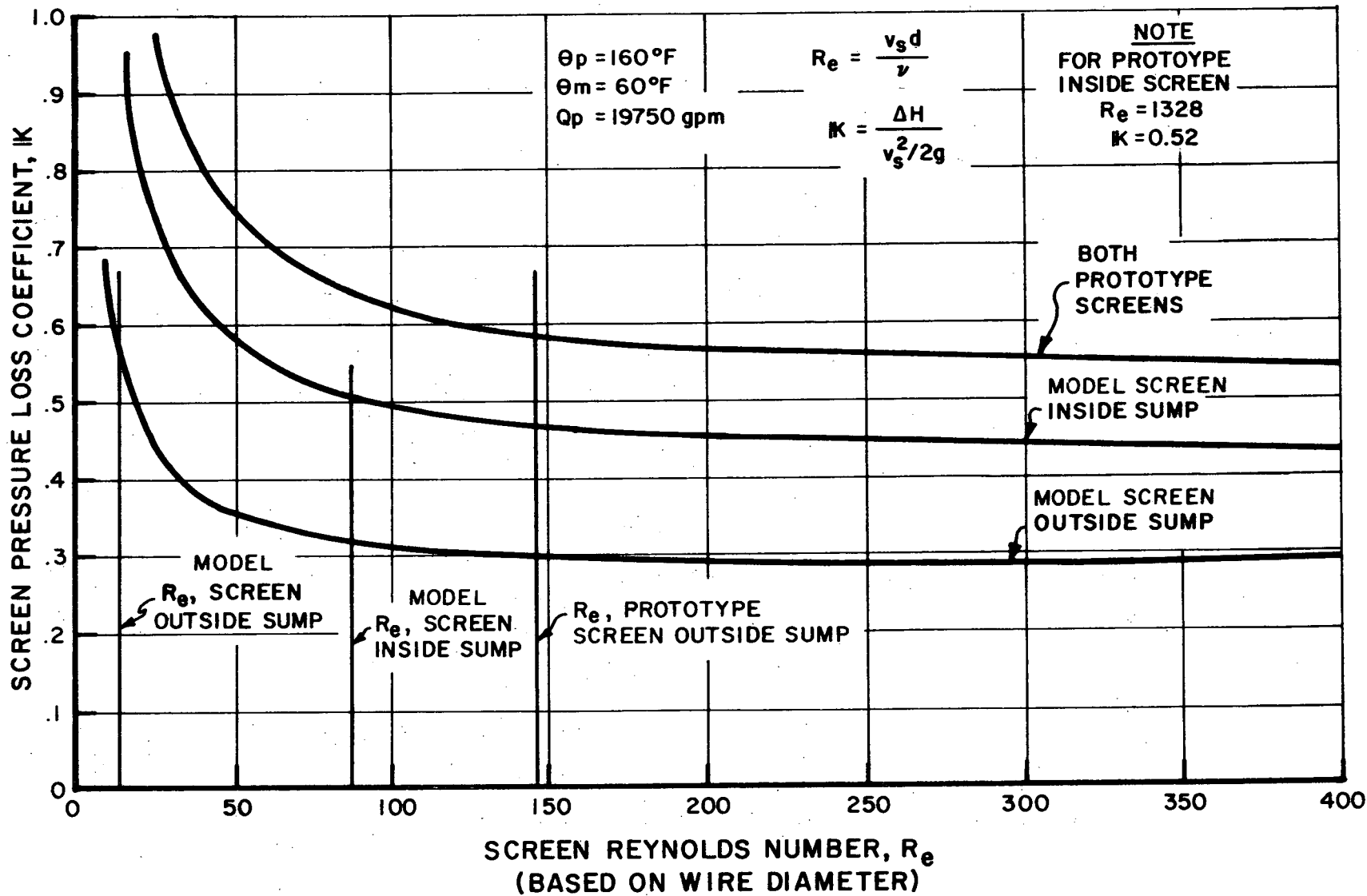


Figure 5 : Loss Coefficient for Screens

Pressure loss coefficients for both prototype and model screens are shown as functions of Reynolds number in Figure 5. Table 2 compares the characteristics of prototype and model screens. It was noted that the sum of the computed head losses through the two screens represented less than five percent of the total sump head loss. Thus the effects of the differences between prototype and model screen pressure loss coefficients on the flow patterns were insignificant.

TABLE 2
COMPARISON OF PROTOTYPE AND MODEL SCREENS
($\theta_p = 160^\circ\text{F}$, $\theta_m = 60^\circ\text{F}$, $Q_p = 19750$ gpm)

Screen	% Open	d (in)	ℓ (in)	K
Prototype, Inside Sump	70.9	.047	.25	.52
Model, Inside Sump	74.6	.017	.108	.50
Prototype, Outside Sump	70.9	.047	.25	.59
Model, Outside Sump	81.0	.025	.225	.56

Sump Loss Coefficient

The sump loss coefficient was determined in the manner of Daily and Harleman⁷ by extrapolating the measured static head in the discharge pipe to the pipe inlet and computing the head loss, h_L , as

$$h_L = \Delta h - V^2/2g$$

where Δh is the static head change between the free water surface and the pipe inlet and $V^2/2g$ is the velocity head in the pipe. The sump loss coefficient was defined as

$$C_L = h_L / (V^2 / 2g)$$

Figure 6 shows a typical evaluation of C_L from pressure gradient data.

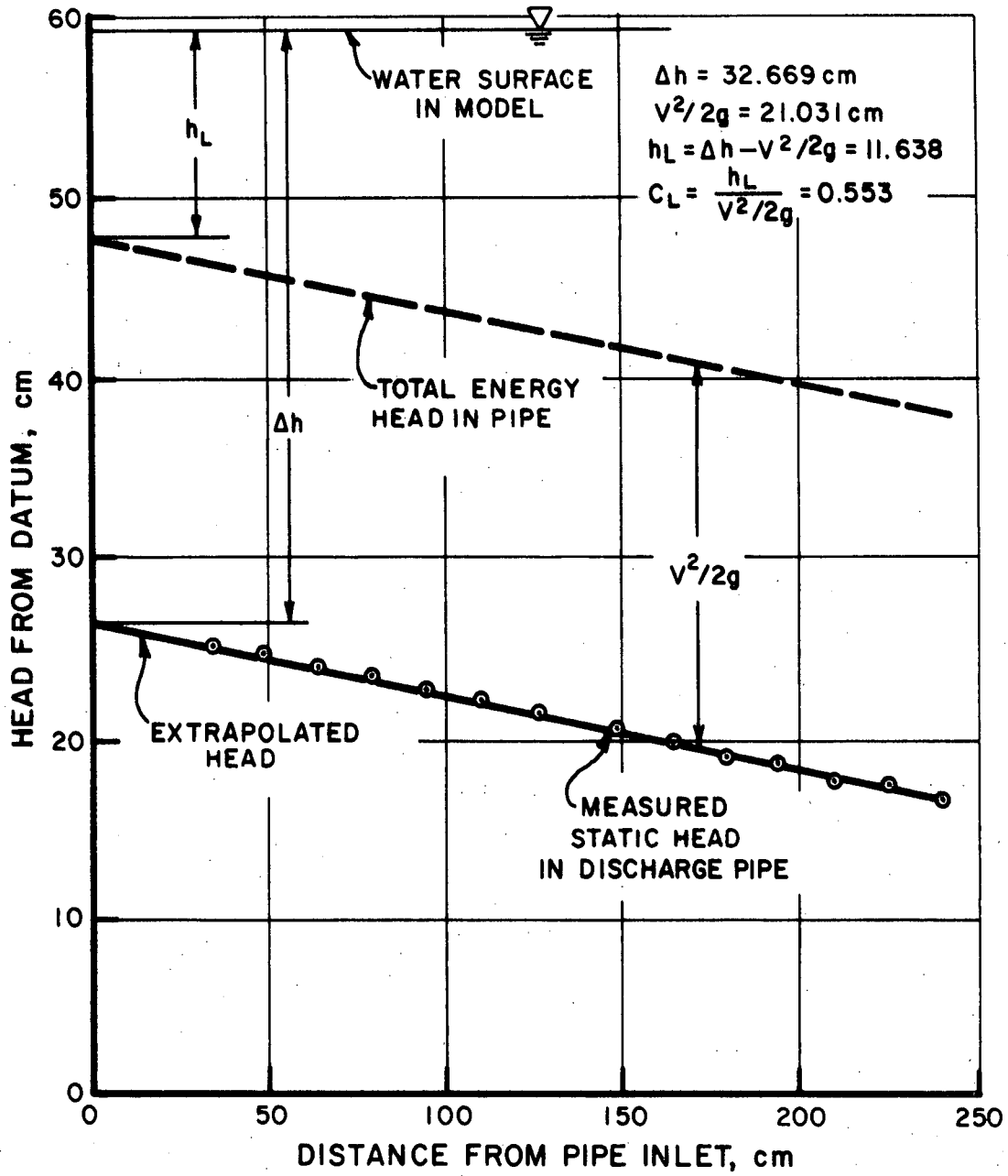


Figure 6 : Illustration of Sump Loss Coefficient Calculation

MODEL TESTS

The final recommended design was developed by performing systematic tests under a variety of flow, geometric, depth, and temperature conditions, with and without vortex suppressors. For each test, the flow patterns were visualized with dye and surface floats. Vortices, if present, were rated according to the arbitrary scale shown in Figure 7. Table 3 shows a summary of the various test conditions using the final design.

RESULTS

Sump Interior

The final recommended design is shown in Figure 8. Because the Watts Bar and Sequoyah sump designs were similar, the vortex suppression and air-release modifications developed for the Sequoyah sump interior were installed in the Watts Bar model before testing began. The performance of these modifications was observed throughout the Watts Bar model testing and found to be satisfactory.

Sump Inlet and Vicinity

With the initial design, a strong vortex (Number 5 in Figure 7) tended to form on the ceiling of the submerged passageway 8 feet above the sump inlet and extend down into the sump. While not quantitatively evaluated, the diameter of this vortex was increased as the size of the air bubble on the ceiling of the passageway increased. This phenomenon was observed at various water depths. The worst case was observed with the water level in the containment lowered to a point where a free surface existed in the passageway.

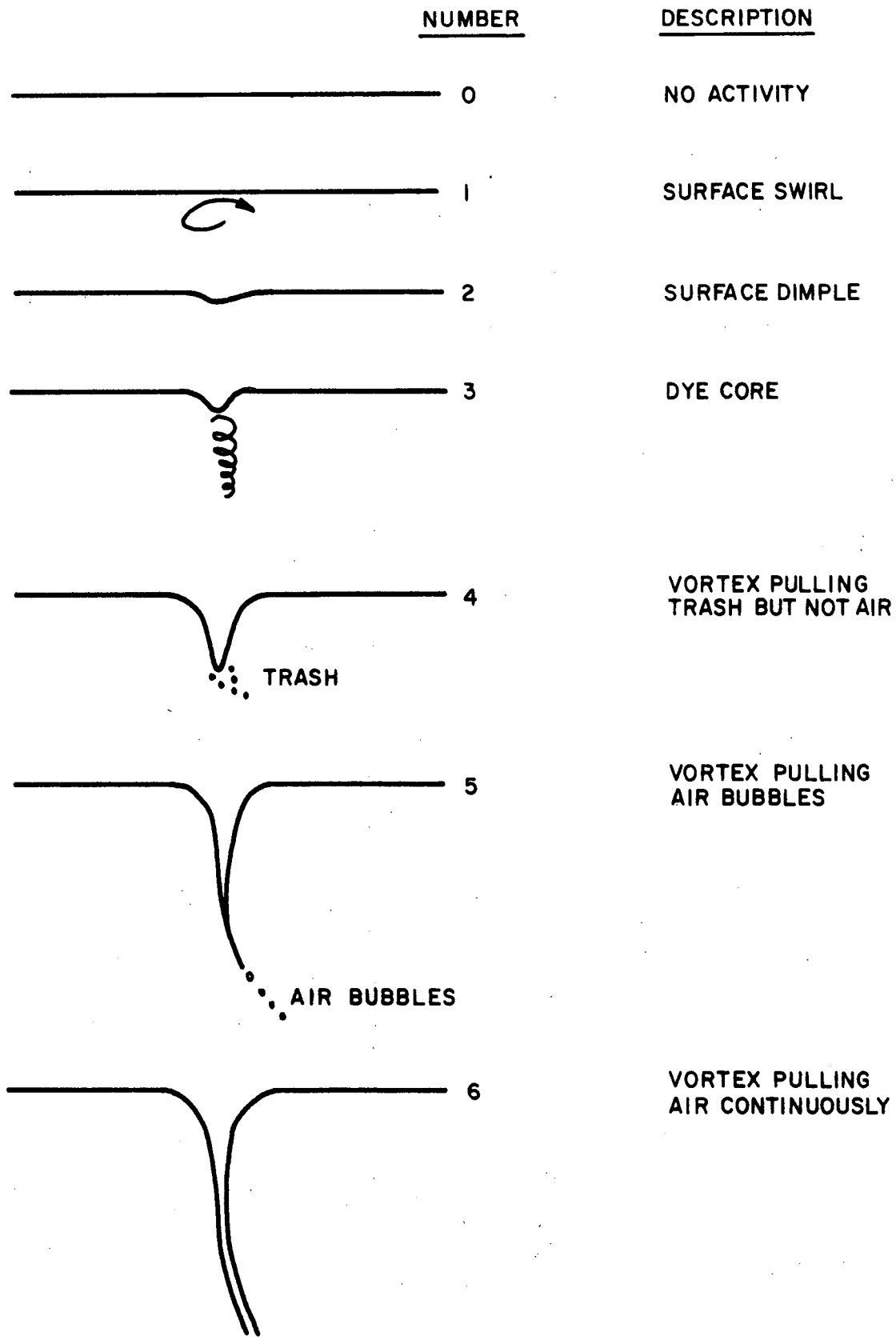


Figure 7 : Arbitrary Vortex Strength Scale

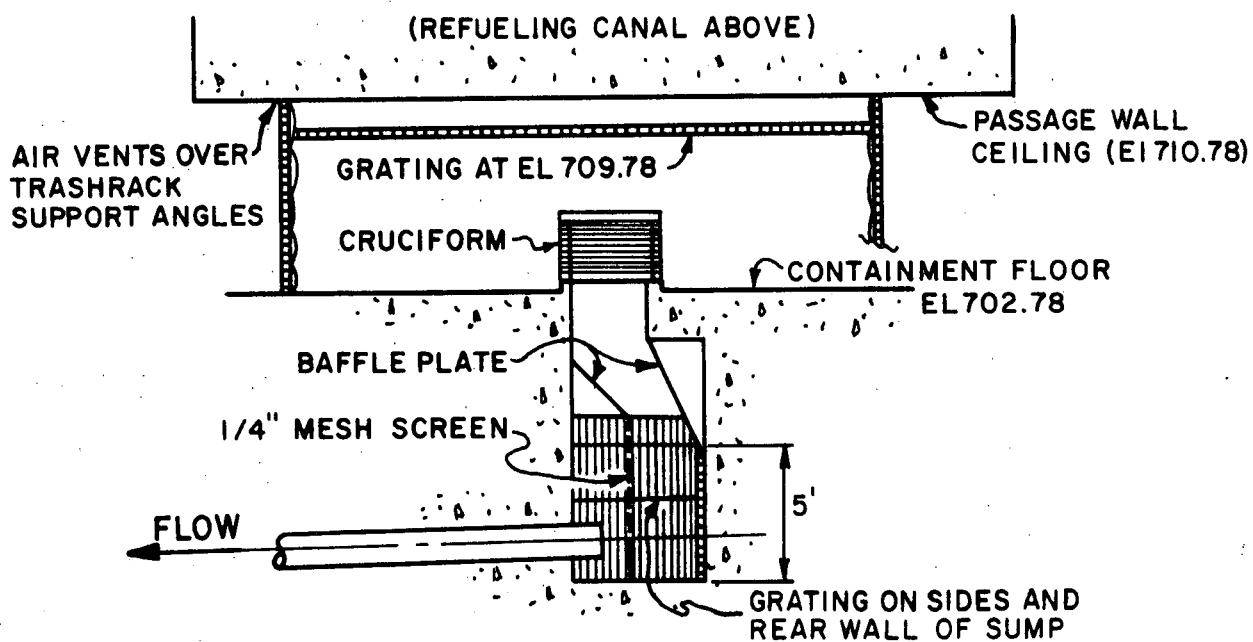
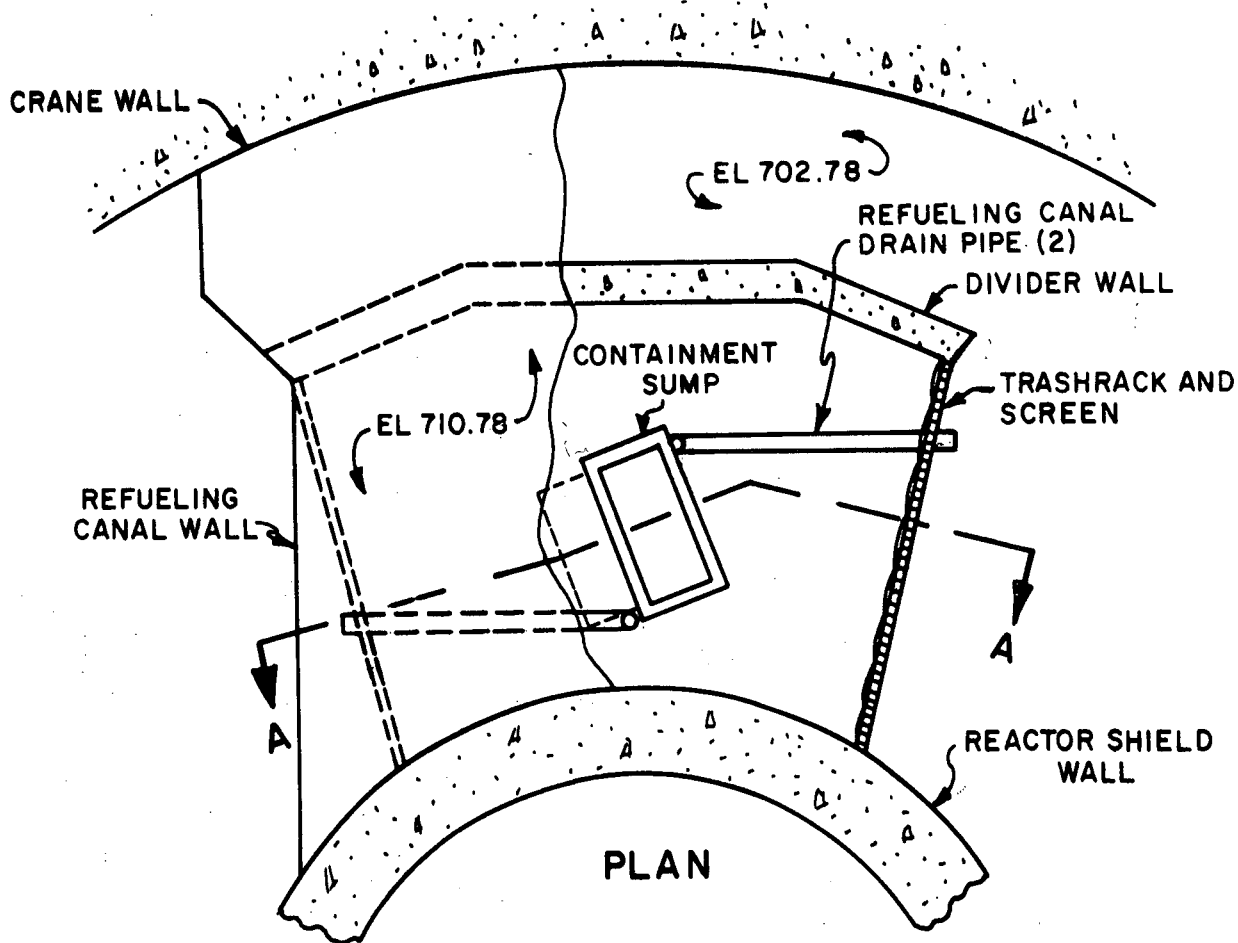
TABLE 3
FINAL DESIGN TEST RESULTS

<u>Test Conditions</u>	<u>Observed Vortex Strength*</u>
Flow Direction**	
Left Side Only	0
Right Side Only	0
Both Sides	0
Flow Rate	
Maximum Possible Model Flow (303% of design flow)	1
Screen Blockage	
Worst Case, 50 percent	0
Water Depth	
Design Depth (13 feet)	0
Reduced Depth (7' 10")	1
Single Pipe Discharge	
Left Pipe Only	0
Right Pipe Only	0

* See Figure 7 for definition

**Looking Downstream

Note: Design water depth and pump flow rate of 19750 gpm (116% of design flow) were used, except where indicated.



SECTION A-A

Figure 8: Final Design with Vortex Suppressors and Other Modifications

Test results showed that this vortexing tendency could be eliminated with the water level at 7'-10" (just below the passageway ceiling) or higher by either (1) suspending standard floor grating one foot below the passageway ceiling or (2) installing a grating-clad cruciform over the sump inlet. For conservatism, both devices were recommended in the final design, as shown in Figure 8. The ceiling grating extended from the reactor shield wall to the divider wall and from trashrack to trashrack. Details of the cruciform are shown in Figure 9. Additionally, the passageway ceiling was vented at the trashracks to get rid of the potential air bubble by placing 3/8" spacer washers between the ceiling and the 3-inch angles supporting the tops of the trashracks as indicated in Figure 8.

Grating used inside the sump had 2-1/2" x 3/16" load bars spaced 1-3/16" on center. Grating used on the cruciform and under the passageway ceiling had 1-1/2" x 3/16" load bars spaced 1-3/16" on center.

Sump Loss Coefficient

The sump loss coefficient, C_L , is shown as a function of discharge pipe Reynolds number in Figure 10. The value of C_L in the prototype at pump design flow rate (17,000 gpm) and design water temperature (160°F) will be about 0.55.

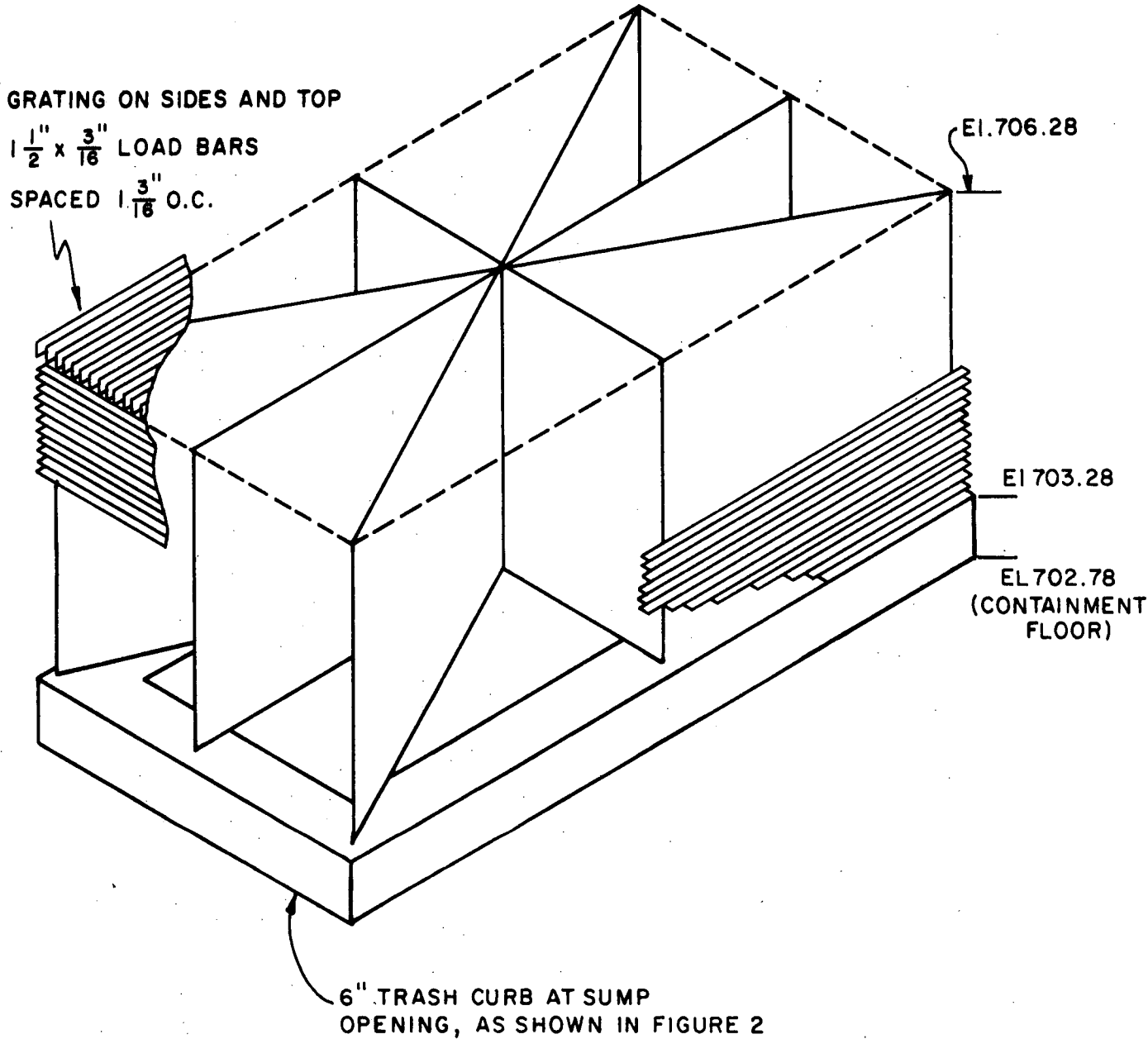


Figure 9 : Details of Cruciform

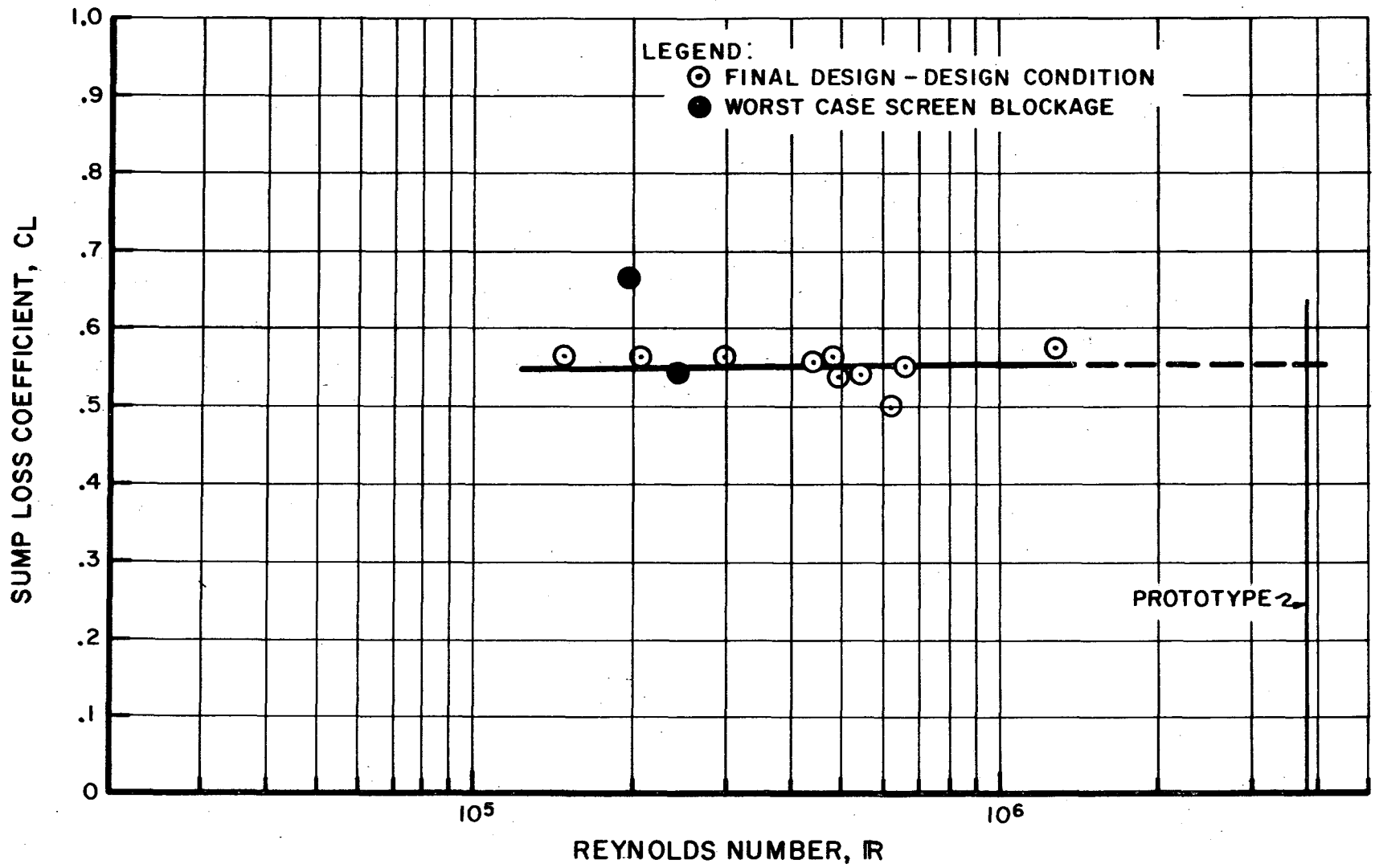


Figure 10: Sump Loss Coefficient Reynolds Number Dependency

CONCLUSIONS

Recommended modifications to the original design are:

- (1) Adoption of the sump internal design developed for the Sequoyah sump
- (2) Installation of grating under the ceiling of the refueling canal for vortex suppression
- (3) Installation of a grating-clad cruciform over the sump inlet for vortex suppression
- (4) Venting of the top trashrack supports at the passageway ceiling for air release.

With these modifications, the sump released all free air during initial filling and gave satisfactory hydraulic performance under all tested conditions.

REFERENCES

1. Pao, Richard H. F., Fluid Mechanics, John Wiley & Sons, 1961.
2. Chang, E., "Review of Literature on Drain Vortices in Cylindrical Tanks," the British Hydromechanical Research Association, Cranfield Bedford, England, TN1342, March 1976.
3. Fain, T. G., "Model Study of the Sequoyah RHR Sump," TVA, Report No. WM28-1-45-102, October 1978.
4. Chang, E., "Review of Literature of the Formation and Modeling of Vortices in Rectangular Pump Sumps," the British Hydromechanical Research Association, Cranfield, Bedford, England, TN1414, June 1977.
5. J. C. Armour, et. al., "Fluid Flow Through Woven Screens," J. AIChE, Vol. 14, No. 3, pp. 415-420, May 1968.
6. Tennessee Valley Authority, "Flow Through Screens," Report No. 87-8, Norris, Tennessee, May 1976.
7. Daily, J. W., and D.R.F. Harleman, Fluid Dynamics, Addison-Wesley, 1965.